

# JAAS

Accepted Manuscript



This is an *Accepted Manuscript*, which has been through the Royal Society of Chemistry peer review process and has been accepted for publication.

*Accepted Manuscripts* are published online shortly after acceptance, before technical editing, formatting and proof reading. Using this free service, authors can make their results available to the community, in citable form, before we publish the edited article. We will replace this *Accepted Manuscript* with the edited and formatted *Advance Article* as soon as it is available.

You can find more information about *Accepted Manuscripts* in the [Information for Authors](#).

Please note that technical editing may introduce minor changes to the text and/or graphics, which may alter content. The journal's standard [Terms & Conditions](#) and the [Ethical guidelines](#) still apply. In no event shall the Royal Society of Chemistry be held responsible for any errors or omissions in this *Accepted Manuscript* or any consequences arising from the use of any information it contains.

1  
2  
3  
4 **A method for improving the accuracy of calibration-free laser-induced**  
5 **breakdown spectroscopy (CF-LIBS) using determined plasma**  
6 **temperature by genetic algorithm (GA)**  
7  
8  
9

10  
11 Juan Dong<sup>1</sup>, Long Liang<sup>1</sup>, Jiao Wei<sup>1</sup>, Hongsheng Tang<sup>1</sup>, Tianlong Zhang<sup>1</sup>,  
12  
13 Xiaofeng Yang<sup>1</sup>, Kang Wang<sup>2</sup>, Hua Li<sup>1\*</sup>  
14  
15  
16

17  
18 The accuracy is still a challenge for classical calibration-free laser-induced  
19  
20 breakdown spectroscopy (CF-LIBS) quantitative analysis since absolute theoretical  
21  
22 calculation and mathematical model cannot compensate for the self-absorption effect  
23  
24 and plasma temperature variability. This research is to obtain more accurate plasma  
25  
26 temperature which contributes to precise elemental composition of unknown samples  
27  
28 for CF-LIBS. Herein, an internal reference-external standard with iteration correction  
29  
30 (IRESIC) method is proposed to correct self-absorption effect and plasma  
31  
32 temperature in CF-LIBS based on internal reference line and one standard sample.  
33  
34 The spectral intensities of each species are corrected by an internal reference line via  
35  
36 iteration procedure, and the internal reference line is suffering from negligible  
37  
38 self-absorption effect for self-absorption correction. Furthermore, one standard  
39  
40 sample matrix-matched with the unknown samples along with the genetic algorithm  
41  
42 (GA) is utilized to simulate the accurate plasma temperature of the unknown samples.  
43  
44 It is worth mentioning that the GA is used for plasma temperature correction through  
45  
46 iteration correction for the first time in CF-LIBS. The proposed method demonstrates  
47  
48 significant improvement in accuracy compared with the classical CF-LIBS in the  
49  
50 quantitative analysis of aluminum-bronze alloy samples due to the integrated merits  
51  
52  
53  
54  
55  
56  
57  
58  
59  
60

of internal reference line usage and accurate plasma temperature evaluation.

## 1. Introduction

Laser induced breakdown spectroscopy (LIBS) technique is a type of emission spectroscopy used for qualitative and quantitative analyses.<sup>1,2</sup> Compared with the conventional analytical techniques, LIBS technique demonstrates the advantages of the capability of fast multi-element synchronous analysis, requiring no sampling or significant sample preparation programs, a strong potential for in situ and real-time analysis, and adaptive capacity to extreme pressure and temperature conditions.<sup>3-8</sup> In the last two decades, LIBS has been successfully applied to quantitative elemental analysis of metals and alloys,<sup>9</sup> artworks,<sup>10</sup> cultural heritage targets,<sup>11</sup> environmental samples,<sup>12</sup> geological samples,<sup>13</sup> bio-medical samples,<sup>14</sup> and nuclear materials.<sup>15</sup> Another inherent advantage of LIBS is the possibility of quantitative elemental analysis of samples with Calibration-free (CF) method. This CF method, proposed by Ciucci et al.<sup>16</sup> in 1999, can be applied to unknown samples<sup>17</sup> or samples where matrix-matched calibration samples are unavailable. The CF-LIBS method was carried out for spectra acquirement on the basis of the following three assumptions: (i) The plasma chemical composition must be the same in the total sample. (ii) The plasma is optically thin.<sup>18,19</sup> (iii) The laser-induced plasma is in local thermodynamic equilibrium (LTE) conditions.<sup>16</sup>

Based on the above assumptions, the theoretical foundation of the CF-LIBS method is described by

$$I_{\lambda}^{ij} = FC_s A_{ij} \frac{g_i}{U_s(T)} e^{-\frac{E_i}{k_B T}} \quad (1)$$

1  
2  
3  
4 where indexes  $i$  and  $j$  refer to upper and lower levels of the transition;  $I$  is integral line  
5  
6 intensity,  $\lambda$  is the particle central wavelength of the transition,  $C_s$  is the number  
7  
8 density of an atomic or ionic species  $s$ ,  $A_{ij}$  is the transition probability between the  
9  
10 two levels,  $g_i$  is the degeneracy of the  $i$  level;  $F$  is a constant that is concerned with  
11  
12 the precise determination of the efficiency of the spectral detection system,  $E_i$  is  
13  
14 energy of the upper level,  $K_B$  is the Boltzmann constant and  $T$  is the plasma electron  
15  
16 temperature,  $U_s(T)$  is the partition function for the emitting species. The spectral  
17  
18 parameters of  $A_{ij}$ ,  $g_i$  and  $E_i$  can be obtained from National Institute for Standards and  
19  
20 Technology (NIST).<sup>20</sup> The values of  $F$ ,  $C_s$  and  $T$  can be determined from the  
21  
22 experimental data.  
23  
24  
25  
26  
27  
28  
29  
30

31 The plasma temperature, usually obtained through the Boltzmann plot method, is  
32  
33 one of the most important parameters for CF-LIBS methods. However, the accuracy  
34  
35 of plasma temperature calculation can be influenced by self-absorption effect,<sup>21-23</sup>  
36  
37 which make the element content and line intensity deviate from the condition of local  
38  
39 thermodynamic equilibrium (LTE), and introduce corresponding errors in Eq.(1). In  
40  
41 recent years, several variants of the classical CF-LIBS method have been reported.  
42  
43 Bulajic et al.<sup>24</sup> in 2002 developed a procedure for correcting self-absorption in  
44  
45 calibration free-laser induced breakdown spectroscopy, their work mainly discusses  
46  
47 about self-absorption corrections in CF-LIBS procedure via a simple  
48  
49 software(LIPS++) which calculates the Curve of Growth (COG) for all the lines.  
50  
51 Internal reference for self-absorption correction (IRSAC), proposed by Sun et al.,<sup>25</sup> is  
52  
53 used for correcting the self-absorption effect which influences accurate determination  
54  
55  
56  
57  
58  
59  
60

1  
2  
3  
4 of plasma temperature. Cavalcanti et al.<sup>26</sup> presented one-point calibration method by  
5  
6 using one standard sample for improving the reliability of quantitative analysis in  
7  
8 CF-LIBS. Calibration-free inverse method was presented in the work of R. Gaudioso  
9  
10 et al.,<sup>27</sup> which is based on an assumption that the temperature determined as described  
11  
12 for a given standard sample can also be assumed for plasmas produced by ablating in  
13  
14 the same conditions other samples of the same kind. The feasibility of inverse method  
15  
16 is demonstrated by comparing the results obtained with classical LIBS.  
17  
18  
19  
20  
21  
22

23 Herein, based on the idea of the above authors, we propose an improved internal  
24  
25 reference-external standard with iteration correction (IRESIC) method to correct  
26  
27 self-absorption effect, calculate plasma temperature, and thus improve the  
28  
29 quantitative performance of the classical CF-LIBS. In this method, an internal  
30  
31 reference line suffering from negligible self-absorption effect for each species is  
32  
33 selected to correct intensities of other spectral lines with self-absorption. One  
34  
35 standard sample matrix-matched with the unknown samples along with the genetic  
36  
37 algorithm (GA) is utilized to simulate the accurate plasma temperature of the  
38  
39 unknown samples.  
40  
41  
42  
43  
44  
45  
46

## 47 **2. Theoretical method of the IRESIC**

48  
49 The concrete algorithm used in the classical CF-LIBS procedure has been  
50  
51 reported in some studies.<sup>16,28</sup> IRESIC method consists of self-absorption correction  
52  
53 and plasma temperature determination, which will be addressed in details in the  
54  
55 following sections.  
56  
57  
58  
59  
60

### **2.1 Model of the self-absorption correction**

Considering the influences of self-absorption on the spectral integrated intensity, a self-absorption coefficient  $b_\lambda$  was introduced here, as expressed in Eq. (1):

$$I_\lambda^{ij} = b_\lambda F C_s A_{ij} \frac{g_i}{U_s(T)} e^{-\frac{E_i}{k_B T}} \quad (2)$$

where the  $b_\lambda$  value is between 0 and 1 ( $b_\lambda=0$  and  $b_\lambda=1$  means the spectral line is absolutely reabsorbed along the optical path and not affected by self-absorption effect, respectively).

The self-absorption effect is corrected by using the internal reference line. Spectral line with lower transition probability and higher excitation energy level is weakly affected by the self-absorption effect, which could be selected as internal reference line. The self-absorption coefficient can be calculated using the intensity ratios of emission line to internal reference line as given by equation (3):

$$b_\lambda = b_{\lambda_R} \frac{I_\lambda^{ij} A_{mn} g_m}{I_{\lambda_R}^{mn} A_{ij} g_i} e^{-\frac{E_m - E_i}{k_B T}} \quad (3)$$

where  $\lambda_R$  is the wavelength,  $I_{\lambda_R}^{mn}$  is spectral line intensity and  $b_{\lambda_R}$  is self-absorption coefficient of the internal reference line, and the  $A_{mn}$ ,  $g_m$  and  $E_m$  are the spectral parameters related to the transition between energy levels of  $m$  and  $n$ . Self-absorption of all the reference lines is assumed negligible (i.e.  $b_{\lambda_R} \approx 1$ ).

Thereby the corrected spectral line intensities can be expressed as:

$$\hat{I}_\lambda^{ij} = \frac{I_\lambda^{ij}}{b_\lambda} = \frac{I_{\lambda_R}^{mn} A_{ij} g_i}{A_{mn} g_m} e^{-\frac{E_m - E_i}{k_B T}} \quad (4)$$

where the line intensity can be corrected by the plasma temperature to obtain a new Boltzmann plot which is used subsequently to renew the temperature. By that logic, such iterative correction is operated until the correlation coefficient converges on the

1  
2  
3  
4 Boltzmann plot. Consequently, a good fitted line will be achieved after initial  
5 self-absorption correction. However, the spectral lines of different species are  
6 affected differently by self-absorption, which leads to inconsistent plasma  
7 temperatures. Hence, it is necessary to carry out further plasma temperature  
8 determination.

## 17 **2.2 Plasma temperature determination with GA**

19  
20 The plasma temperature of the standard sample is determined by GA which is  
21 used to search an optimal temperature between minimum and maximum. As an  
22 adaptive heuristic search algorithm, GA is put forward based on the natural selection  
23 and genetics conjecture.<sup>29</sup> The fundamental idea of GA aims at simulating the natural  
24 evolution process, especially referring to that of “the survival of the fittest” raised by  
25 Darwin. To be specific, by the operation of reproduction, crossover and mutation  
26 generated the next generation of the species, whose individuals (binary-encoded  
27 strings) were compared due to the difference of their fitness, and the result is that  
28 individuals with high fitness are given a greater chance to “reproduce” offspring,  
29 while ones with low fitness are less likely to get selected for reproduction and “die”  
30 eventually. By the same token, it refers to an intelligent development of a random  
31 search in a defined search space to optimize and tackle the issue.<sup>30, 31</sup>

32  
33  
34  
35  
36  
37  
38  
39  
40  
41  
42  
43  
44  
45  
46  
47  
48  
49  
50  
51  
52 Considering a reasonable balance between accuracy and computational effort, the  
53 tuning parameters of the GA method are as follows: sp(population size)=7,  
54 pc(crossover probability)=0.5, pm(mutation probability)=0.2, in(number of  
55 iterations)= 120.

1  
2  
3  
4 In GA process, an individual corresponds to a temperature. A random population  
5  
6 of individuals is initialized between minimum and maximum temperatures, and the  
7  
8 random temperatures can be converted to binary number, respectively, for fitness  
9  
10 evaluation. Each temperature is used to calculate composition of each species based  
11  
12 on CF-LIBS, different individuals in the GA population create different average  
13  
14 relative error between the calculated and the actual concentrations, then a linear  
15  
16 transformation operation is introduced to adjust the average relative error so as to  
17  
18 ensure the best offspring, the adjusted average relative error is fitness. Random  
19  
20 parents are selected from the current population using roulette wheel selection. For  
21  
22 the recombination of the genetic population, the genetic operators like crossover and  
23  
24 mutation are applied to the parents, and then the fitness given by the objective  
25  
26 function are evaluated and compared to select the best individuals. The best  
27  
28 individuals can be determined by an iterative procedure until the maximum  
29  
30 generation number is reached. A full procedure of the GA was described in  
31  
32 reference.<sup>32,33</sup> In general, GA efficiently cope with non-linear mixed/integer  
33  
34 optimization problems with constraints, which can be input constraints or the  
35  
36 constrains of the process states.<sup>32</sup>  
37  
38  
39  
40  
41  
42  
43  
44  
45  
46  
47  
48

49  
50 Based on a confirmed and reasonable assumption in reference<sup>27,34</sup> that plasmas of  
51  
52 different samples of similar typology and ablated in the same conditions have the  
53  
54 same temperatures, the temperature obtained with the GA can be applied to the set of  
55  
56 unknown samples to evaluate their composition. The flow diagram of the IRESIC is  
57  
58 described in Fig. 1.  
59  
60

### 3. Experimental Methods

#### 3.1 Experimental Setup

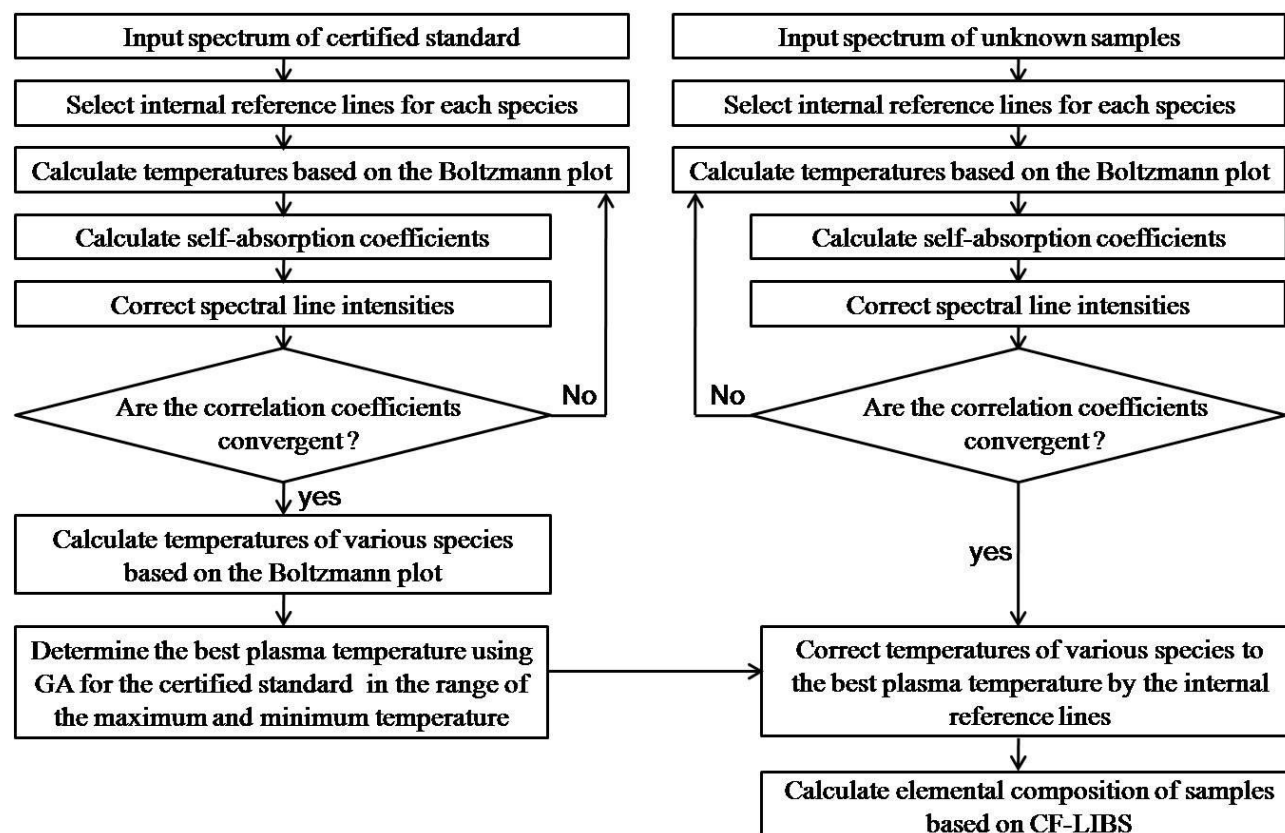


Fig.1 Flow diagram of the proposed IRESIC method

All LIBS measurements were performed with the Nd: YAG laser (LOTIS, T II 2131, Belarus), which has an output energy of 61mJ ( $4.3 \text{ GW/cm}^2$ ) at 1064 nm with a repetition rate of 10 Hz, and the details of this LIBS system were described in reference.<sup>35</sup> The spectral range of 220-800 nm was covered by an Echelle spectrometer (LTB, ARYELLE 150, Germany). An electron-multiplying CCD camera (QImaging, UV enhanced,  $1004 \times 1002$  pixels, USA), was coupled to the spectrometer and used for the detection of dispersed light. A mechanical chopper was used in front of the entrance slit to prevent the CCD from detecting the early plasma continuum. The LIBS measurement was carried out under the atmosphere condition,

and the gate width of spectrometer was set to 2ms. Single-pulse measurements were conducted with a delay of 2  $\mu$ s between the firing of the laser and recording of the spectrum.

### 3.2 Materials

Five aluminum-bronze alloy standard samples (BYG1916-1, CHINALCO LUOYANG COPPER CO., LTD) were purchased as samples to verify the IRESIC approach to the CF-LIBS procedure. The size of the purchased standard copper alloy is: 1#( $\Phi$  30  $\times$  40 mm), 2#( $\Phi$  30  $\times$  40 mm), 3#( $\Phi$  30  $\times$  40 mm), 4#( $\Phi$  30  $\times$  40 mm), 5#( $\Phi$  30  $\times$  40 mm). To fit the size of sample compartment, the five aluminum-bronze alloy standard samples ( $\Phi$  30  $\times$  6 mm) were obtained at the same positions from each sample. Table 1 reported the size and composition of five aluminum-bronze alloy samples. 1# sample as one standard sample was used to obtain the accurate plasma temperature, the others were considered as unknown samples.

**Table 1** Mass composition (in wt. %) of five aluminum bronze alloy samples

Sample	Sample Size	Al	Fe	Mn	Pb	Sn	Si	Ni	Zn	As	Sb	P	Cu
1#	$\Phi$ 30 $\times$ 6 mm	7.76	4.94	2.63	—	—	—	—	—	—	—	—	84.67
2#	$\Phi$ 30 $\times$ 6 mm	8.78	4.17	2.92	—	—	—	—	—	—	—	—	84.13
3#	$\Phi$ 30 $\times$ 6 mm	9.75	3.51	2.01	—	—	—	—	—	—	—	—	84.73
4#	$\Phi$ 30 $\times$ 6 mm	9.24	3.01	1.56	0.0043	0.051	0.13	0.25	0.69	0.020	0.0048	0.0067	84.99
5#	$\Phi$ 30 $\times$ 6 mm	9.14	3.17	1.57	0.068	0.033	0.19	0.15	1.11	0.033	0.0076	0.0048	84.52

### 3.3 Data Acquisition

LIBS spectra from 50 different locations of each sample surface are gathered. A measured spectrum was obtained by accumulation of 20 laser shots in per location for the purpose of improving the signal-to-noise ratio. In order to minimize the influence from sample heterogeneity and other fluctuations, every 5 measured spectra at

different locations were averaged into an analytical spectrum. Fig. 2 shows a representative spectrum of sample 1# measured by LIBS system. The data processing and quantitative analysis for aluminum-bronze alloy standard samples by chemometrics methods were carried on Matlab(version 2010a, Mathworks).

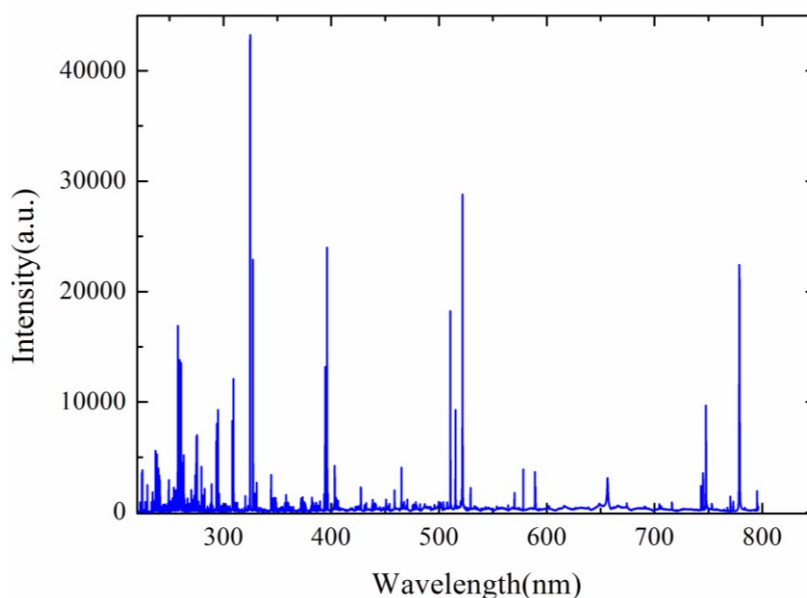


**Fig.2** A representative spectrum of sample 1# obtained by the proposed LIBS system

## 4. Results and Discussion

### 4.1 Selection of analytical lines

Under specific LIBS measurement conditions, all the analytical lines are selected on the basis of NIST database<sup>20</sup> and reference.<sup>36</sup> The emission lines from atoms and ions of each element usually are considered. Particularly, if the number of ionized lines is too little, only atomic lines are selected. However, the accuracy of the quantitative results of the CF-LIBS method is often influenced by the self-absorption effect, especially for the major elements. In this paper the emission lines have been selected according to following criteria:

(1) The lines involved in the ground state should be excluded for the possibility of

self-absorption influence. For high concentration elements, lines corresponding to transitions with lower energy level below 0.74eV have also not been selected.<sup>37</sup>

**Table 2** List of the selected emission lines used for building the Boltzmann plot

Species	Wavelength(nm)							
Al	236.72	237.33	265.27	266.05	305.49	305.74	306.44	308.23
	309.29	394.41	396.17					
Cu	282.45	296.12	330.79	360.20	427.55	465.17	510.60	521.86
	578.23							
Fe I	258.47	269.91	270.86	272.61	278.82	305.74	309.99	347.56
	349.04	353.36	355.86	357.01	358.12	361.88	363.15	364.79
	373.48	374.95	375.83	376.39	376.73	380.67	381.59	382.04
	382.59	383.43	384.11	385.00	404.60	427.20	438.37	532.83
Fe II	234.82	235.46	235.91	236.87	236.99	239.27	239.93	240.49
	241.80	242.43	242.83	243.29	243.49	244.47	245.46	245.89
	246.02	246.19	246.34	246.40	246.52	246.96	247.08	248.27
	249.33	249.91	250.36	251.19	251.44	251.92	252.55	252.97
	253.37	253.57	253.90	254.89	256.70	258.61	259.95	261.40
	266.48	266.69	268.48	269.28	270.42	271.46	272.77	273.71
	274.33	274.66	274.95	277.94	278.38	294.41	298.49	300.28
Mn I	259.58	276.12	281.81	288.30	302.27	304.33	304.58	307.04
	309.71	322.83	323.67	325.60	333.05	354.78	357.01	357.78
	358.67	360.89	380.95	382.36	383.43	384.11	392.65	397.61
	398.53	401.82	404.15	405.57	405.90	408.37	411.10	425.79
	428.42	449.04	449.91	476.27	476.66	478.39	482.39	496.56
	519.67	525.52	534.95	581.68	601.39	602.22	698.90	728.41
Mn II	243.80	249.91	251.69	253.57	254.36	255.68	255.87	255.95
	256.37	260.58	261.04	261.83	262.58	263.83	265.12	265.61
	267.28	268.07	269.33	269.55	270.19	270.59	270.86	271.05
	271.18	272.47	281.52	281.65	287.02	287.30	287.96	288.68
	288.97	289.25	289.89	293.94	294.92	303.11	303.55	305.07
	344.21	346.04	347.41	348.30	348.88	349.58	349.76	

(2) Lines with lesser transition probability below  $2 \times 10^6 \text{ s}^{-1}$  are supposed to be eliminated.

(3) All the interference and deformation spectral lines should be weeded out.

(4) To avoid larger calculation error caused by the fluctuations of individual lines, the number of the selected analytical lines should not be too little.

All the selected emission lines are summarized in Table 2.

**Table 3** The selected internal reference lines for all samples

Species	Wavelength/nm
Al I	305.49
Cu I	465.17
Fe I	349.04
Fe II	242.43
Mn I	404.15
Mn II	270.86

In the IRESIC method, the selection of the internal reference line plays a key role in the whole procedure, selecting one single reference line for each species to correct other lines reflect in a large uncertainty on the results, due to different species suffer from different self-absorption effects and radiation mechanisms. Therefore, an analytical line with less self-absorption effect should be selected as the internal reference line. Furthermore, the priority should be given to the lines of upper levels with high excitation energies, low transition probabilities and appropriate spectral intensity to avoid moderate intensity saturation. It should be point out that different reference lines are required to different spectrum according to the acquisition time parameters and experimental conditions. The internal reference lines for all samples in this study are listed in Table 3.

#### 4.2 Correction of self-absorption effect with internal reference line

In this research, the self-absorption effect is corrected for all the test samples. The Boltzmann plots before and after initial correction of the IRESIC method on the

reference sample 1# is shown in Fig. 3.

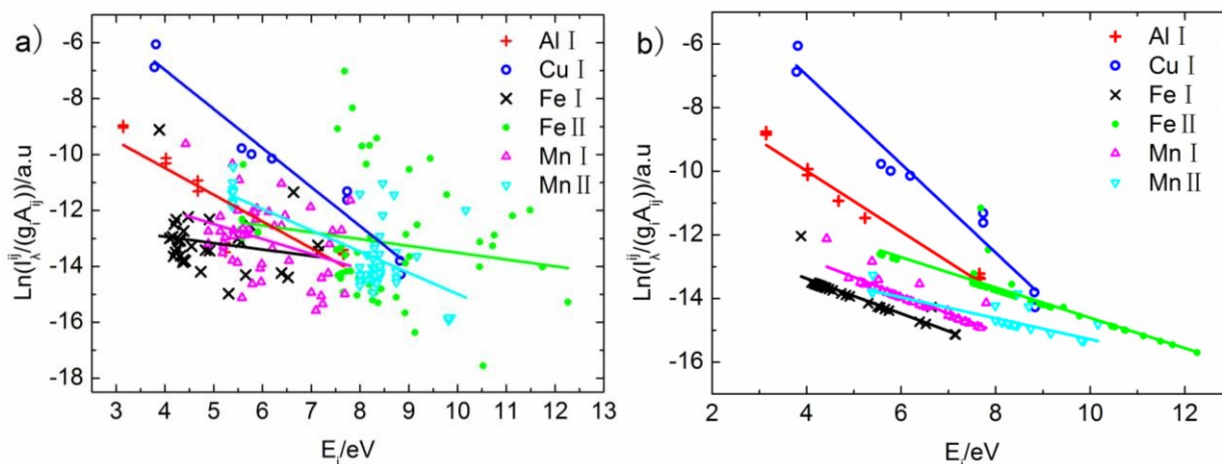


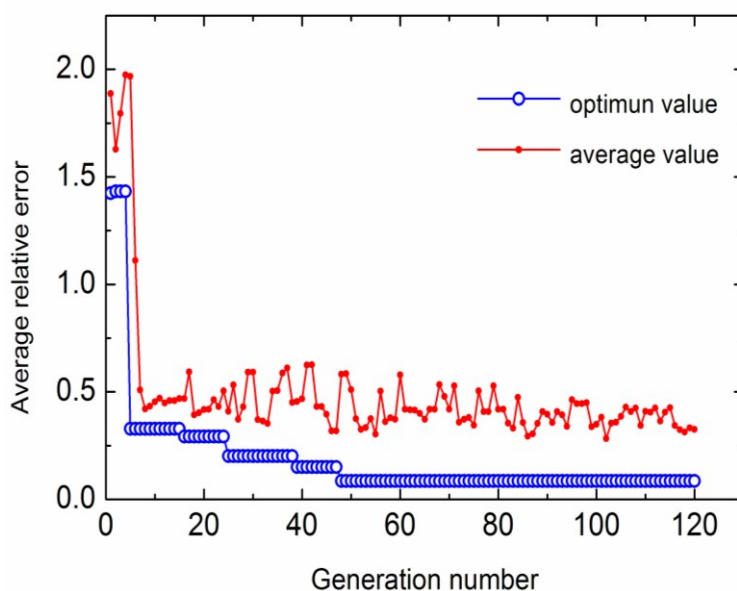
**Fig. 3** Boltzmann plots before and after self-absorption initial correction by the IRESIC method for 1# sample (a) before correction (b) after correction

As shown in Fig. 3, points on the Boltzmann plots demonstrate randomly scattered distribution as well as poor linear regression before correction. The reason is that dramatic decrease of intensity for most spectral lines, the decrease of slope and intercept of regression lines for each species caused by self-absorption. Accordingly, the calculating temperature exceeds the actual temperature significantly. These points are distributed near the regression line after initial correction with the IRESIC method, however, the slope of each regression line is inconsistent indicating that the self-absorption has different effect on the spectral intensities of the different species. Moreover, the self-absorption of all the reference lines do not be evaluated, but just is assumed to be negligible.

#### 4.3 Determination of the plasma temperature with one standard sample

The calculated maximum and minimum temperature are 35116K and 8313K, respectively. The optimal temperature close to the real plasma temperature could be obtained by the GA between 8313K and 35116K. In the GA process, a random

1  
2  
3  
4 population of individuals is initialized, the size of the population can be seven  
5  
6 individuals per generation. Through evaluating the fitness for all the initial  
7  
8 individuals of the population, random parents are selected from the population with  
9  
10 roulette wheel selection. In order to avoid trapping in local optimum, the genetic  
11  
12 operators like crossover and mutation are applied to parents for a new generation.  
13  
14 The temperature corresponded to best fitness is optimal plasma temperature. Fig. 4  
15  
16 shows the optimization procedure of GA, where the ordinate with fitness is converted  
17  
18 to the average relative error for the purpose of easy observation and discussion.  
19  
20  
21  
22  
23  
24



25  
26  
27  
28  
29  
30  
31  
32  
33  
34  
35  
36  
37  
38  
39  
40  
41  
42  
43  
44  
45  
46  
47  
48  
49  
50  
51  
52  
53  
54  
55  
56  
57  
58  
59  
60

**Fig. 4** The optimization procedure of Genetic algorithm

From Fig. 4, the average relative error decreases when iterations increase, and finally stabilize. It shows that in the initial population, the best individuals failed to obtain from the population. Subsequently, the best parent genes are selected to ensure the best offspring, the new individuals are generated by performing operation like crossover and mutation from the population. With the increase of iterations, the best individuals in growing numbers can be inherited. For running about 50-120 times, the

1  
2  
3  
4 optimum value tends to stabilization, which indicates average relative error  
5  
6  
7 corresponding to the optimal temperature is 12086K (called the plasma temperature),  
8  
9  
10 also means an iteration stopping criterion which is adopted to avoid computing the  
11  
12 time.

13  
14  
15 The fact that Boltzmann plots provide an individual temperature for each species,  
16  
17  
18 and the desired temperature is limited to a range (8313 - 35116K). Thus, in the  
19  
20 IRESIC method the optimal temperature can be regarded as a representative reference  
21  
22 value of energy distribution of various species in the plasma phase,<sup>33</sup> not real  
23  
24 temperature of the plasma or excitation temperature of a species.  
25  
26

#### 27 28 **4.4 Application to unknown samples** 29

30  
31 Here, a verified assumption proposed that plasmas produced by ablating in the  
32  
33 same conditions different samples of the same kind have the same temperature. The  
34  
35 validity of this assumption was discussed and further verified in reference.<sup>27,33</sup> Using  
36  
37 the temperature determined with the GA from one standard sample it is reasonable to  
38  
39 calculate the composition of the other four unknown samples by applying the usual  
40  
41 CF-LIBS procedure. The Boltzmann plots, determined by the classical CF-LIBS  
42  
43 method and IRESIC method, are shown in Figs.5-8. From Figs. 5, 6, 7 and 8, it can  
44  
45 be observed that the distribution of the points and lines on Boltzmann plots are  
46  
47 scattered before correction. After correction, all the fitting lines tend to parallel, and  
48  
49 the temperature corresponded to the slope is in close proximity to the estimated value  
50  
51 of plasma temperature. After correction, all the fitting lines tend to parallel, and  
52  
53 the temperature corresponded to the slope is in close proximity to the estimated value  
54  
55 of plasma temperature.  
56  
57  
58  
59  
60

Table 4 shows the quantitative results obtained by the classical CF-LIBS and our

**Table 4** Quantitative results for 1#, 2#, 3#, 4# and 5#samples calculated in present work

element	Concentration (wt%)			Relative standard deviation (%)	
	Certified value	Classical CF-LIBS	IRESIC	Classical CF-LIBS	IRESIC
1# sample					
Al	7.76	1.13	7.35	85.44	5.24
Cu	84.67	98.47	84.63	16.30	0.05
Fe	4.94	0.04	4.84	99.34	2.08
Mn	2.63	0.36	3.18	86.31	21.06
2# sample					
Al	8.78	3.17	10.30	63.90	17.21
Cu	84.13	96.52	82.65	14.73	1.76
Fe	4.17	0.02	4.22	99.41	1.09
Mn	2.92	0.29	2.84	90.07	2.75
3# sample					
Al	9.75	2.64	9.08	72.92	6.88
Cu	84.73	96.82	84.92	14.27	0.23
Fe	3.51	0.07	3.91	97.90	11.50
Mn	2.01	0.46	2.09	77.11	3.80
4# sample					
Al	9.24	4.40	9.31	52.38	0.74
Cu	84.99	71.92	80.80	97.74	4.73
Fe	3.01	1.96	3.65	34.88	21.10
Mn	1.56	1.60	1.80	2.56	15.21
Other elements	1.20	20.12	4.44	—	—
5# sample					
Al	9.14	3.32	9.89	63.68	8.21
Cu	84.52	65.02	81.60	23.07	3.45
Fe	3.17	1.31	3.76	58.68	18.61
Mn	1.57	1.19	1.63	24.20	3.82
Other elements	1.60	29.16	3.12	—	—

proposed IRESIC method. The main discrepancies between the two methods are shown in table for elemental concentrations of samples. In the case of the classical CF-LIBS method, the calculated element mass concentration is grossly incorrect. However, in IRESIC method, lines of all samples are corrected using an internal reference line, which helps to improve linear relation on the Boltzmann plot.

But different slopes of regression lines hinder determination of the accurate temperature, then the plasma temperature was obtained with the GA for one standard sample, we employ it to calculate elemental compositions of unknown samples. As a result of the application of the IRESIC method, the concentrations calculated on the unknown samples are remarkably close to the actual concentrations, accuracy of quantitative analysis of the IRESIC method is greatly improved for major element, and the relative error is reduced greatly, but it has a large deviation for minor elements. Yet it is important to note that the temperature determined by one certified standard is not absolutely the same as real temperature of the plasma. Moreover, the CF-LIBS method is based on the idea of concentration normalization. Thus the quantitative results of major element of a certain species will affect the results of minor elements, which is embodied in content of minor element Pb、Sn、Si、Ni for sample 4# and sample 5#.

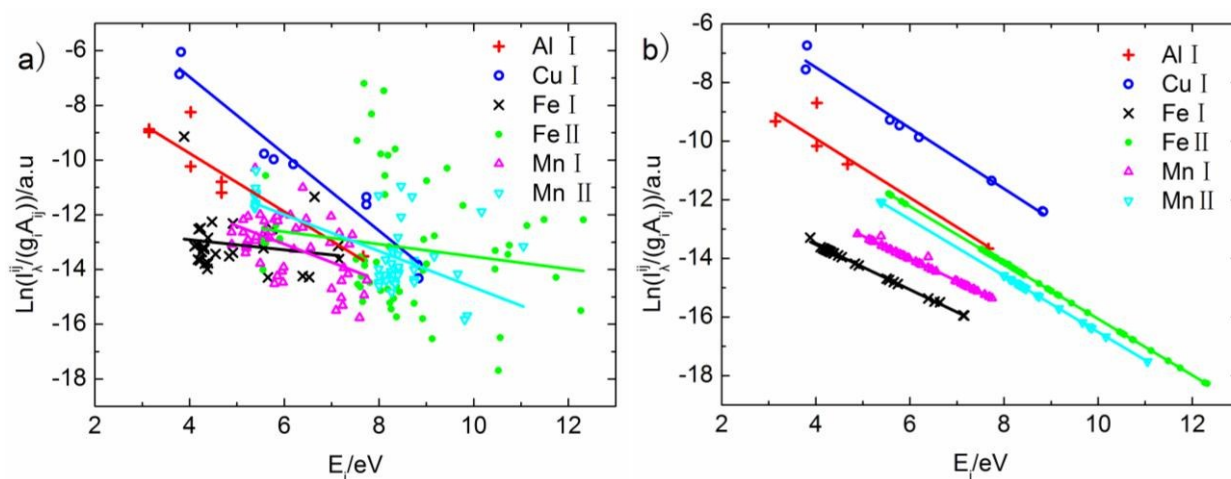


**Fig. 5** Boltzmann plots before and after corrected by the IRESIC method for 2# sample (a) before correction (b) after correction

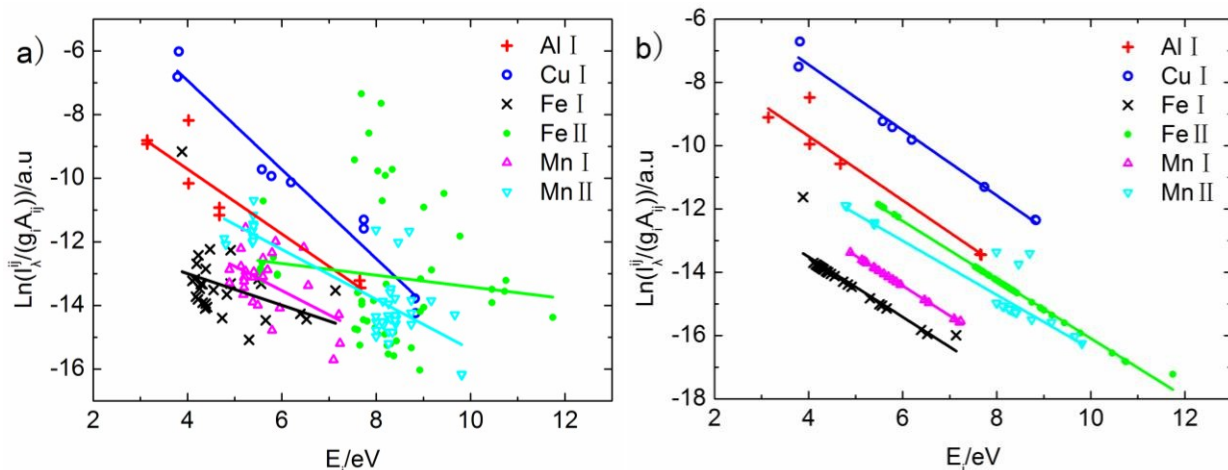


**Fig. 6** Boltzmann plots before and after corrected by the IRESIC method for 3# sample (a) before correction (b) after correction

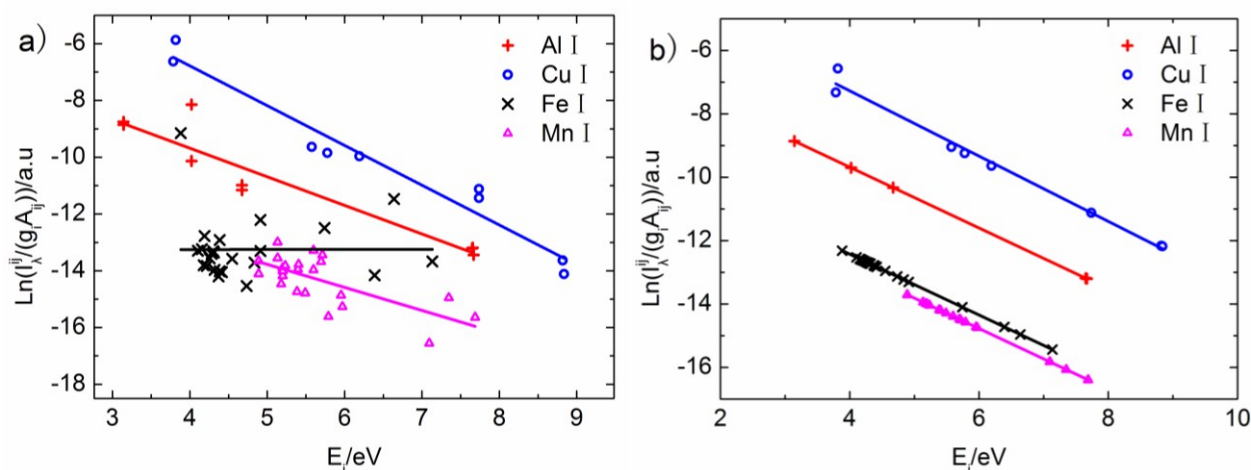


**Fig. 7** Boltzmann plots before and after corrected by the IRESIC method for 4# sample (a) before correction (b) after correction

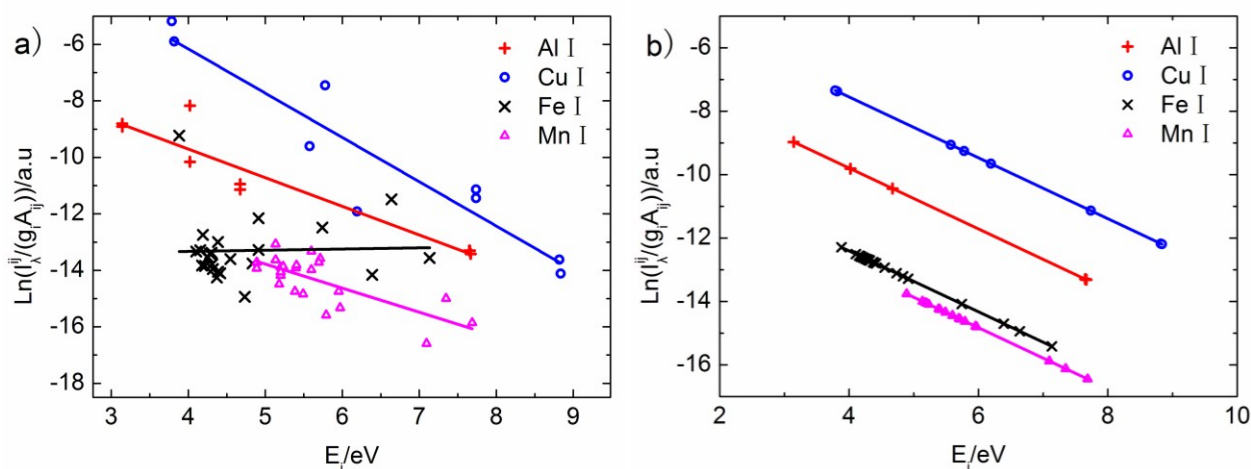


**Fig. 8** Boltzmann plots before and after corrected by the IRESIC method for 5# sample (a) before correction (b) after correction

1  
2  
3  
4  
5  
6  
7  
8  
9  
10  
11  
12  
13  
14  
15  
16  
17  
18  
19  
20  
21  
22  
23  
24  
25  
26  
27  
28  
29  
30  
31  
32  
33  
34  
35  
36  
37  
38  
39  
40  
41  
42  
43  
44  
45  
46  
47  
48  
49  
50  
51  
52  
53  
54  
55  
56  
57  
58  
59  
60

## 5. Conclusion

In summary, an improved method for CF-LIBS is proposed based on the idea of internal reference conjugated with external standard. The IRESIC method is not only used for correcting the spectral intensities of each species by an internal reference line, but also calculating the plasma temperature by using one standard sample and GA. The calculated plasma temperature value is directly used as the one of matrix-matched unknown samples. The GA based approach with a restricted parameter setting for the fitness evaluation produced more accurate plasma temperature for temperatures between the minimum and maximum. The efficiency of the modified CF-LIBS method is validated by comparing its quantitative analysis results of the copper alloy with the ones obtained through the classical CF-LIBS method. The modified CF-LIBS method show that the results obtained through its application are more precise than the ones obtained using a classical CF-LIBS method. In addition, one standard sample used in the IRESIC method improve the feasibility and reliability in in situ and real-time LIBS analysis, providing a theoretical basis for the further promotion and application site LIBS analysis techniques.

## Acknowledgements

This research was supported by the National Natural Science Foundation of China (No. 21375105 and No. 21175106), the National Major Scientific Instruments and Equipment Development Projects of China (2011YQ030113), Research Fund for the Doctoral Program of Higher Education of China (No. 20126101110019), and

Scientific Research Plan Project of Shaanxi Education Department (No.14JK1746).

## Notes and references

<sup>1</sup>*Institution of Analytical Science, College of Chemistry & Materials Science, Northwest University, Xi'an, 710069, China. Fax: Tel: 86-029-88302635; E-mail: nwufxkx2012@126.com*

<sup>2</sup>*College of Science, Chang'an University, Xi'an, 710064, China*

1. D.W. Hahn, N. Omenetto, *Applied Spectroscopy*, 2010, **64**, 335A-366A.
2. D.W. Hahn, N. Omenetto, *Applied Spectroscopy*, 2012, **66**, 347-419.
3. F.J. Fortes, J. Moros, P. Lucena, L.M. Cabalín, J.J. Laserna, *Analytical Chemistry*, 2013, **85**, 640-669.
4. A. De Giacomo, M. Dell'Aglio, R. Gaudiuso, S. Amoroso, O. De Pascale, *Spectrochimica Acta Part B-Atomic Spectroscopy*, 2012, **78**, 1-19.
5. R. Noll, *Laser-Induced Breakdown Spectroscopy*, Springer-Verlag, Berlin Heidelberg, 2012.
6. R. Gaudiuso, M. Dell'Aglio, O. De Pascale, G.S. Senesi, A. De Giacomo, *Sensors*, 2010, **10**, 7434-7468.
7. J.P. Singh, S.N Thakur (Eds.), *Laser-Induced Breakdown Spectroscopy*, Elsevier, 2007.
8. A.M. Miziolek, V. Palleschi, I. Schechter (Eds.), *Laser-induced breakdown spectroscopy (LIBS)*, Cambridge: Cambridge University Press, 2006.
9. A. De Giacomo, M. Dell'Aglio, R. Gaudiuso, A. Santagata, G.S. Senesi, M. Rossi, M.R. Ghiara, F. Capitelli, O. De Pascale, *Chemical Physics*, 2012, **398**, 233-238.
10. V. Burakov, V. Kiris, A. Klyachkovskaya, N. Kozhukh, S. Raikov, *Microchimica Acta*, 2007, **156**, 337-342.
11. A. Giakoumaki, K. Melessanaki, D. Anglos, *Analytical and Bioanalytical Chemistry*, 2007, **387**, 749-760.
12. F. Capitelli, F. Colao, M.R. Provenzano, R. Fantoni, G. Brunetti, N. Senesi, *Geoderma*, 2002, **106**, 45-62.
13. B. Salle, D. A. Cremers, S. Maurice, R. C. Wiens, *Spectrochimica Acta Part B-Atomic Spectroscopy*, 2005, **60**, 479-490.
14. O. Samek, D. C. S. Beddows, H. H. Telle, G. W. Morris, M. Liska, J. Kaiser, *Applied Physics A: Materials Science & Processing*, 1999, **69**, S179-S182.
15. M.Z. Martin, S. Allman, D.J. Brice, R.C. Martin, N.O. Andre, *Spectrochimica Acta Part B-Atomic Spectroscopy*, 2012, **74-75**, 177-183.
16. A. Ciucci, M. Corsi, V. Palleschi, S. Rastelli, A. Salvetti, E. Tognoni, *Applied Spectroscopy*, 1999, **53**, 960-964.
17. K.K. Herrera, E. Tognoni, I. B. Gornushkin, N. Omenetto, B.W. Smith, J.D. Winefordner, *Journal of Analytical Atomic Spectrometry*, 2009, **24**, 426-438.
18. N. Konjević, *Physics Reports*, 1999, **316**, 339-401.
19. N. Konjević, M. Ivković, S. Jovicević, *Spectrochimica Acta Part B-Atomic Spectroscopy*, 2010, **65**, 593-602.
20. <http://physics.nist.gov/PhysRefData/Handbook/periodictable.htm>.
21. F. Bredice, F.O. Borges, H. Sobral, M. Villagran-Muniz, H.O. Di Rocco, G. Cristoforetti, S. Legnaioli, V. Palleschi, A. Salvetti, E. Tognoni, *Spectrochimica Acta Part B-Atomic Spectroscopy*, 2007, **62**, 1237-1245.

- 1  
2  
3  
4  
5  
6  
7  
8  
9  
10  
11  
12  
13  
14  
15  
16  
17  
18  
19  
20  
21  
22  
23  
24  
25  
26  
27  
28  
29  
30  
31  
32  
33  
34  
35  
36  
37  
38  
39  
40  
41  
42  
43  
44  
45  
46  
47  
48  
49  
50  
51  
52  
53  
54  
55  
56  
57  
58  
59  
60
22. A.M. El Sherbini, Th.M. El Sherbini, H. Hegazy, G. Cristoforetti, S. Legnaioli, V. Palleschi, L. Pardini, A. Salvetti, E. Tognoni, *Spectrochimica Acta Part B-Atomic Spectroscopy*, 2005, **60**, 1573-1579.
  23. F. Bredice, F.O. Borges, H. Sobral, M. Villagran-Muniz, H.O. Di Rocco, G. Cristoforetti, S. Legnaioli, V. Palleschi, L. Pardini, A. Salvetti, E. Tognoni, *Spectrochimica Acta Part B-Atomic Spectroscopy*, 2006, **61**, 1294-1303.
  24. D. Bulajic, M. Corsi, G. Cristoforetti, S. Legnaioli, V. Palleschi, A. Salvetti, E. Tognoni, *Spectrochimica Acta Part B-Atomic Spectroscopy*, 2002, **57**, 339-353.
  25. L.X. Sun, H.B. Yu, *Talanta*, 2009, **79**, 388-395.
  26. G.H. Cavalcantia, D.V. Teixeiraa, S. Legnaiolib, G. Lorenzettib, L. Pardinib, V. Palleschib, *Spectrochimica Acta Part B-Atomic Spectroscopy*, 2013, **87**, 51-56.
  27. R. Gaudiuso, M. Dell'Aglio, O. De Pascale, S. Loperfido, A. Mangone, A. De Giacomo, *Analytical Chimica Acta*, 2014, **813** 15-24.
  28. I.B. Gornushkin, N. Omenetto, B.W. Smith, J.D. Winefordner, *Applied Spectroscopy*, 2004, **58**, 1023-1031.
  29. M.J.C. Pontes, R.K.H. Galvão, M.C.U. Araújo, P.N.T. Moreira, O.D.P. Neto, G.E. José T.C.B. Saldanha, *Chemometrics and Intelligent Laboratory Systems*, 2005, **78**, 11-18.
  30. D. Jouan-Rimbaud, D.L. Massart, R. Leardi, O.E. De Noord, *Analytical Chemistry*, 1995, **67**, 4295-4301.
  31. R. Leardi, *Journal of Chemometrics*, 2001, **15**, 559-569.
  32. K. Man, K. Tang, S. Kwong, Genetic algorithms, concepts and designs, *Springer-Verlag*, 1998.
  33. J. Causa, G. Karer, A. Núñez, D. Sáez, I. Škrjanc, B. Zupančič, *Computers and Chemical Engineering*, 2008, **32**, 3254-3263.
  34. R. Gaudiuso, M. Dell'Aglioc, O. De Pascalea, A. Santagatac, A. De Giacomo, *Spectrochimica Acta Part B-Atomic Spectroscopy*, 2012, **74-75**, 38-45.
  35. L. Liang, T.L. Zhang, K. Wang, H.S. Tang, X.F. Yang, X.Q. Zhu, Y.X. Duan, H. Li, *Applied Optics*, 2014, **53**, 544-552.
  36. R. Kurucz, CD-ROM No.23, Harvard-Smithsonian Center for Astrophysics, 1995.
  37. A. De Giacomo, M. Dell'Aglio, O. De Pascale, S. Longo, M. Capitelli, *Spectrochimica Acta Part B-Atomic Spectroscopy*, 2007, **62**, 1606-1611.